

# Saharan Dust Transport and High-Latitude Glacial Climatic Variability: The Alboran Sea Record

Ana Moreno

*CRG Marine Geosciences, Department of Stratigraphy, Paleontology and Marine Geosciences, Faculty of Geology, University of Barcelona, Campus de Pedralbes, C/Martí i Franqués, s/n°, E-08028 Barcelona, Spain*

Isabel Cacho<sup>1</sup>

*CRG Marine Geosciences, Department of Stratigraphy, Paleontology and Marine Geosciences, Faculty of Geology, University of Barcelona, Campus de Pedralbes, C/Martí i Franqués, s/n°, E-08028 Barcelona, Spain; and Department of Environmental Chemistry (ICER-CSIC), Jordi Girona, 18, 08034 Barcelona, Spain*

Miquel Canals<sup>2</sup>

*CRG Marine Geosciences, Department of Stratigraphy, Paleontology and Marine Geosciences, Faculty of Geology, University of Barcelona, Campus de Pedralbes, C/Martí i Franqués, s/n°, E-08028 Barcelona, Spain*

Maarten A. Prins

*Faculty of Earth Sciences, Vrije Universiteit, De Boelelaan 1085, 1081 HV Amsterdam, The Netherlands*

María-Fernanda Sánchez-Goñi

*EPHE, Département Géologie et Océanographie, UMR-CNRS 5805, University Bordeaux I, France*

Joan O. Grimalt

*Department of Environmental Chemistry (ICER-CSIC), Jordi Girona, 18, 08034 Barcelona, Spain*

and

Gert Jan Weltje

*Department of Applied Earth Sciences, Delft University of Technology, P.O. Box 5028, NL-2600 GA Delft, The Netherlands*

Received January 9, 2002

Millennial to submillennial marine oscillations that are linked with the North Atlantic's Heinrich events and Dansgaard–Oeschger cycles have been reported recently from the Alboran Sea, revealing a close ocean-atmosphere coupling in the Mediterranean region. We present a high-resolution record of lithogenic fraction variability along IMAGES Core MD 95-2043 from the Alboran Sea that we use to infer fluctuations of fluvial and eolian inputs to the core site during periods of rapid climate change, between 28,000 and 48,000 cal yr B.P. Comparison with geochemical and pollen records from the same core enables end-member compositions to be determined and to document fluctuations of fluvial and eolian inputs on millennial and faster timescales. Our data document increases in

northward Saharan dust transports during periods of strengthened atmospheric circulation in high northern latitudes. From this we derive two atmospheric scenarios which are linked with the intensity of meridional atmospheric pressure gradients in the North Atlantic region. © 2002 University of Washington.

**Key Words:** Saharan dust; Dansgaard–Oeschger cycles; Heinrich events; Mediterranean region; end-member modelling; teleconnections.

## INTRODUCTION

Paleoclimatic records from a wide range of marine and terrestrial archives document rapid fluctuations during the last glacial and provide compelling evidence that the so-called Dansgaard–Oeschger (D/O) oscillations and Heinrich cold events (HE) were of global significance (i.e., Leuschner and Sirocko, 2000). This millennial-scale variability has been attributed to instabilities in

<sup>1</sup> Present Address: University of Cambridge, The Godwin Laboratory, Pembroke Street, Cambridge CB2 3SA, U.K.

<sup>2</sup> To whom correspondence should be addressed. Fax: +34 93 402 13 40. E-mail: miquel@natura.geo.ub.es.

the ocean thermohaline circulation and associated marine heat transports (Broecker, 1994; Zahn *et al.*, 1997). While the driving force behind these oscillations remains unclear, evidence is mounting that sporadic meltwater injections to the Atlantic Ocean, perhaps with a stochastic component, may play a primary role in causing these ocean–climate swings (Boyle, 2000; Ganopolski and Rahmstorf, 2001).

Besides a probable ocean component, atmospheric circulation changes have also been suggested as a possible mechanism to explain the close correlation of the millennial ocean and climate signals over long distances. Indications of an intensified atmospheric circulation during cold stadial periods is contained within dust records from the Greenland ice cap (Mayewski *et al.*, 1994) as well as in paleoceanographic records that document monsoonal variability (Leuschner and Sirocko, 2000; Schulz *et al.*, 1998) and the Chinese loess record (An, 2000; Porter and Zhisheng, 1995). The apparent interhemispheric coupling in conjunction with the indication of rapid reorganizations of atmospheric circulation (Fuhrer *et al.*, 1999) may imply a global atmospheric signal superimposed on regional climatic changes, themselves caused by thermohaline switches or ice dynamics.

In view of the increasing paleoclimatic database and, in particular, because of their potential societal relevance, it becomes increasingly important to better understand the underlying mechanisms that drove the D/O cycles and to gain better control on the timing and potential asynchrony of these climatic oscillations between low and high latitudes (Peterson *et al.*, 2000).

Because of its midlatitude position the Mediterranean region is a key location to investigate climatic connections between high and low latitudes. In addition, its landlocked nature in conjunction with the only limited water exchange with the open ocean makes the Mediterranean Sea particularly sensitive to environmental changes. Recent studies of marine and lacustrine sediment records from the Mediterranean area have shown a strong correlation with the Greenland ice-core records (Allen *et al.*, 1999; Cacho *et al.*, 1999; Sánchez-Goñi *et al.*, 2002). For instance, the indication of rapid changes of deep-water convection in the western Mediterranean at the pace of the North Atlantic D/O cycles has been used to infer likewise rapid changes of northwesterly winds which are the main forcing mechanism for thermohaline overturn in the region (Cacho *et al.*, 2000). These studies demonstrate that Mediterranean climates and marine circulation on millennial scales were closely coupled with the North Atlantic ocean–atmosphere system.

IMAGES Core MD 95-2043 in the Alboran Sea, western-most Mediterranean, is located at a midlatitude position that is influenced by high-latitude and subtropical wind systems and thus provides the unique opportunity to study phase relations of millennial-scale climate variations between low and high latitudes (Fig. 1). Paired records of grain-size and geochemical variability together with pollen records along this core enable temporal relations between marine and terrestrial systems to be determined without the dating uncertainties that are normally encountered in studies where such records are derived from

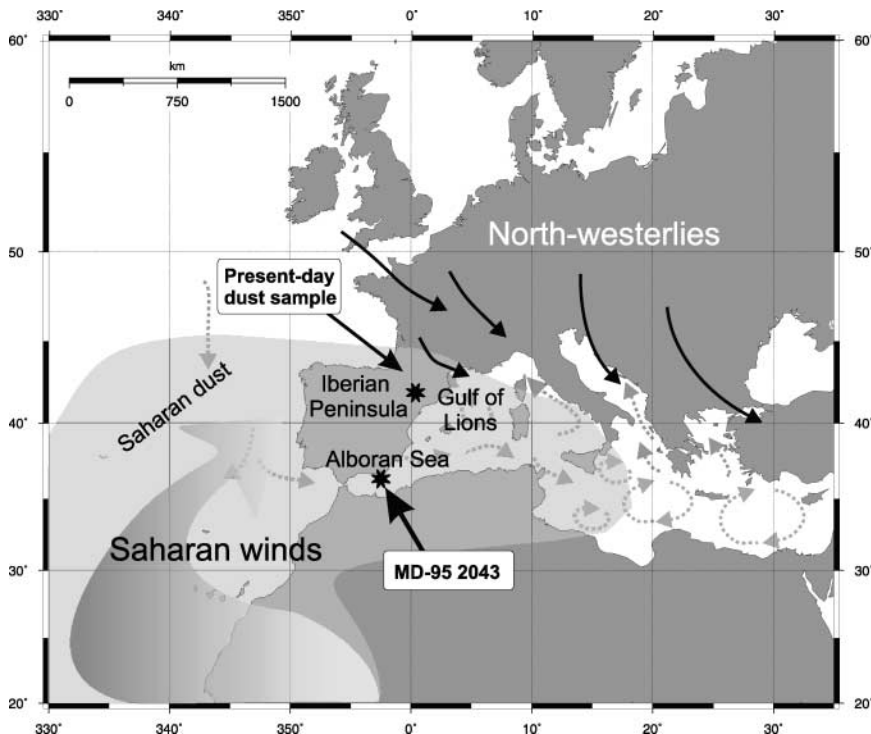


FIG. 1. Location of IMAGES core MD 95-2043 in the Alboran Sea. Black arrows indicate the mean positions of north-westerlies and thick arrow represents dust-bearing Saharan winds. Present-day oceanographic circulation is represented by dashed arrows. Also shown is the location of the station where present-day Saharan dust samples were recovered. The grey cloud represents a typical dust outbreak over the Western Mediterranean.

several cores or archives. This allows a better understanding of the underlying mechanisms that drive millennial-scale climatic variability.

## STUDY AREA

The Mediterranean Sea acts as a concentration basin in which evaporation exceeds freshwater input through precipitation and runoff (Béthoux, 1979). The Alboran Sea constitutes the Mediterranean's westernmost basin and through the Strait of Gibraltar provides the gateway for water exchange with the Atlantic (Fig. 1). Summertime climates usually are dry and hot in this region due to the influence of the atmospheric subtropical high-pressure belt (Sumner *et al.*, 2001). During winter the subtropical high is shifted to the south, allowing midlatitude storms to enter the region from the open Atlantic and bringing enhanced amounts of rainfall to the Mediterranean. Anomalous torrential rainfalls occur during this season in response to severe storms that are generated locally by extreme atmospheric convective overturn (Romero *et al.*, 1999). Much of the present-day climate variability in this region on a decadal timescale has been linked to a natural mode of atmospheric pressure variation, the North Atlantic Oscillation (NAO; Rodó *et al.*, 1997). NAO activity is indexed as the difference between normalized winter sea-level atmospheric pressure between the Azoric high-pressure and Icelandic low-pressure cells such that a high NAO index is derived from a strong meridional pressure gradient that results in the North Atlantic depression tracks to follow a more northerly route. During low NAO index years, northwesterly winds are weaker and are guided to midlatitudes, thus bringing higher precipitation to the Mediterranean and large areas of North Africa. There is increasing observational evidence for some degree of interlinking between the NAO variability and North Atlantic physical circulation so that an influence of North Atlantic thermohaline circulation on regional weather patterns cannot be ruled out (Hurrell, 1995; Dickson, 1997).

The interplay between Saharan air masses and the Azoric high-pressure cell constitutes another meteorological pattern that defines Mediterranean climates. Evaluation of back trajectories and isobaric meteorological maps shows that Sahara air masses dominate the Mediterranean region whenever the Azores High is displaced westward and the North African High is strengthened and centered over Algeria (Rodríguez *et al.*, 2001). The development of summertime thermal lows over the Iberian Peninsula apparently stimulates this meteorological setting through intense heating of the land surface.

The contribution and deposition of terrigenous sediments in the Alboran Sea is closely linked with the regional meteorological patterns. Primary routes for the transportation of lithogenic particles to the Alboran Sea is through fluvial sediment transport and airborne dust. Supply of fluvial particles from the southern Iberian Peninsula is favored by torrential local rainfalls and a scarce vegetation cover that supports surficial erosion, while fluvial sediment transport from the northern African margin seems to be negligible (Fabrès *et al.*, 2002). Eolian transport of dust from the Sahara is well known as an important contributor to

marine sediments and the northward and north-eastward transport of dust off North Africa seems almost as important as the dust flux into the Atlantic (Ganor and Foner, 1996). Saharan dust deposition over the western Mediterranean has been estimated at  $9\text{--}25 \text{ t} \cdot \text{km}^{-2} \cdot \text{yr}^{-1}$  which represents 10–20% of the recent deep-sea sedimentation (Guerzoni *et al.*, 1997). An eolian sedimentation rate of  $23 \text{ g} \cdot \text{m}^{-2} \cdot \text{yr}^{-1}$  has been reported for continental southeastern Iberia (Díaz-Hernández and Miranda Hernández, 1997), equivalent to 12% of the lithogenic particle flux recently collected in a sediment trap experiment in the Alboran Sea (Fabrès *et al.*, 2002). These results underscore the importance of eolian sediment supply as an inherent component of Alboran Sea sediments and its value as tracer of regional climate variability during the past.

## MATERIAL AND METHODS

IMAGES Core MD 95-2043 was retrieved in 1995 in the western Alboran Sea ( $36^{\circ}8.6'N$ ;  $2^{\circ}37.3'W$ ) at a water depth of 1841 m (Fig. 1). We use the age model that was developed by Cacho *et al.* (1999) for this core, which is derived from graphically correlating the down-core  $U_{37}^{K'}$  sea surface temperature (SST) record with the D/O climatic cycles displayed in the Greenland GISP2 ice core  $\delta^{18}O$  record (Meese *et al.*, 1997). According to this age model the records presented in this study, from 1025 to 1585 cm core depth, span the time interval from 28,000 to 48,000 cal yr B.P.

Grain-size distribution was measured at 5-cm intervals after removing organic matter from the bulk sample through oxidation with 10%  $H_2O_2$  and leaching the carbonate fraction with an ammonium acetate solution that was buffered at a pH of 4.0. Sediment samples with and without the carbonate fraction were analyzed with a Coulter LS 100 Laser Particle Size Analyser (CLS), which determines particle grain sizes between 0.4 and 800  $\mu\text{m}$ . CLS precision and accuracy were tested by several control runs using latex micro-spheres with a defined diameter. The high precision (reproducibility) of the measurements is demonstrated by small variations in the mean diameter (0.97% of variation) and in the standard deviation (1.37% of variation). Accuracy of the measurements as indicated by the relative departure from the nominal mean diameter is 0.30%, corresponding to absolute deviations between 0.09 and 0.34  $\mu\text{m}$ . Additional test runs were performed using microsphere assemblages with mixed grain-sizes to ensure the CLS accurately determines poly-modal grain-size distributions.

To aid in the interpretation of the grain-size records, we modeled end-member grain-size distributions using the down-core CLS measurements and applying the numerical-statistical algorithms developed by Weltje (1997; see also Prins and Weltje, 1999). Grain-size end-members represent a series of fixed sediment grain-size compositions that can be regarded as discrete subpopulations within the data set from all analyses. We derived grain-size end-members from data that were obtained from carbonate- and organic-fraction-free samples so as to not have our interpretations obscured by processes that are unrelated to lithogenic sediment transport and deposition.

We obtained control values for present-day eolian dust grain sizes from a sample collected during a red rainfall event (March 24, 1991) at La Castanya (Montseny Mountains, 41°46'N, 2°21'E; Fig. 1). The sample was filtered with Millipore 0.45- $\mu\text{m}$  pore-size filters, dried at 100°C, and analyzed with the CLS (Avila, 1996).

Chemical analysis of the sediment samples was performed through X-ray fluorescence using a Philips PW 2400 sequential wavelength disperse X-ray spectrometer. Prior to analysis all samples were ground and homogenized in an agate mortar. Glass discs were prepared for major element determination by fusing about 0.3 g of ground bulk sediment with a Li-tetraborate flux.

Analytical accuracy was checked by measuring international standards. Precision of individual measurements was better than 0.8% as determined from replicate analyses of samples.

## RESULTS

### Grain-Size Distribution

The SST record along IMAGES core MD95-2043 displays millennial-scale variability that is closely related to the Greenland ice-core D/O cycles, as has been previously reported by Cacho *et al.* (1999) (Fig. 2a). The median of the two sets of

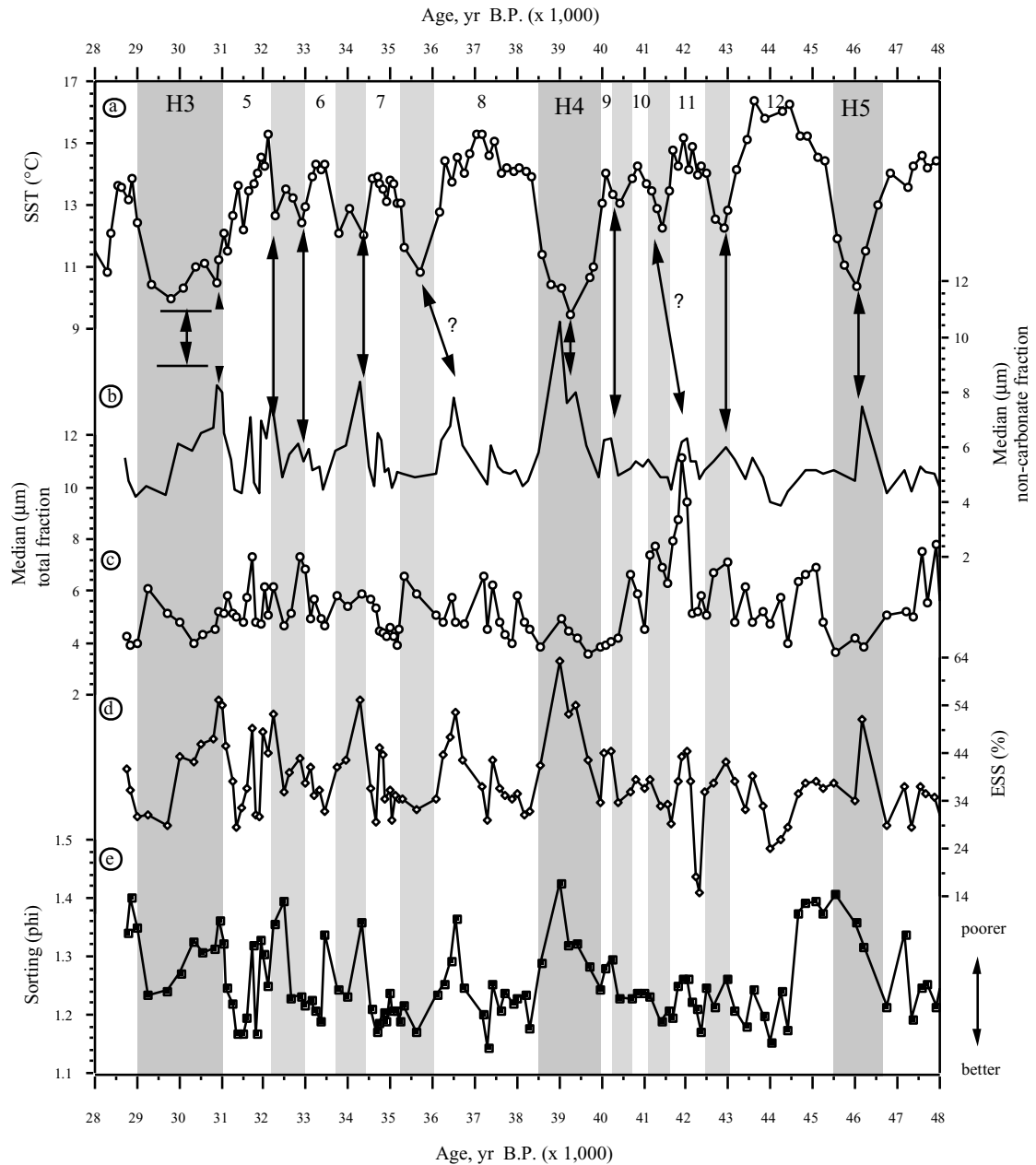


FIG. 2. Time series of (a) SST estimation based on Cacho *et al.* (1999) and grain-size parameters: (b) median (non-carbonate fraction), (c) median (total fraction), (d) "Eolian Sortable Silt" (ESS) content, and (e) sorting. HE and D/O stadial periods are indicated by shaded bars following GISP2 age model (Meese *et al.*, 1997), and D/O interstadial periods are indicated by numbers. Arrows mark correlation of grain-size maxima and cold stadial periods.

samples analyzed, with and without carbonate, is calculated and plotted versus age (Fig. 2b, 2c). This median represents the grain-size distribution midpoint. The different pattern of both records prevents any common interpretation in terms of transport mechanisms. Median grain size of the carbonate-free fraction varies between 4 and 11  $\mu\text{m}$ , with maximum grain sizes occurring during the HE (Fig. 2b). The correlation with the D/O cyclicity is best developed in this record in the interval between HE3 and HE4, 29–40 cal yr B.P.

The Eolian sortable silt (ESS) fraction has been defined by McCave *et al.* (1995) as the percentage of the sediment in the 7- to 63- $\mu\text{m}$  size range. ESS represents the sediment fraction susceptible to be transported by wind whereas the size fraction below 7  $\mu\text{m}$  is influenced by particle scavenging through rainfall without a measurable size dependence (McCave *et al.*, 1995). In our records there is no indication of a significant lithogenic component in the sand fraction  $>63 \mu\text{m}$ , and thus we use the entire sediment fraction  $>7 \mu\text{m}$  as representing the ESS. The results obtained show a pattern of variation similar to the previous grain-size parameters for the terrigenous fraction, that is, closest correlation with the D/O pattern in the period between HE4 and HE3 (Fig. 2d).

Another grain-size parameter that we consider in this study is the sediment sorting index as defined by McManus (1988) (Fig. 2e). The record reveals cyclic variations from poorly sorted sediment during colder periods to better sorting during warmer periods. Such correlation is in conflict with previously reported data that demonstrate enhanced sediment grain-size sorting during periods of increased eolian sediment contribution (i.e., Lamy *et al.*, 1998).

### Grain-Size End-Member Model

*Estimating the number of end-members.* End-member modelling of grain-size distributions has been carried out to improve our interpretation of the observed grain-size variations. To estimate the minimum number of end-members required for a satisfactory approximation of our grain-size data, the coefficient of determination,  $r^2$ , was calculated. This coefficient represents the proportion of variance of each grain-size class that can be reproduced by the approximated data (Weltje, 1997; Prins and Weltje, 1999).  $r^2$  when plotted against grain size allows for several end-member solutions to be determined (Fig. 3). With the two end-member model ( $r^2$  mean = 0.5; Fig. 3c) only the fractions between 3 and 5  $\mu\text{m}$  and 20 and 40  $\mu\text{m}$  are adequately explained ( $r^2 > 0.8$ ). In the three end-member model ( $r^2$  mean = 0.81) the majority of grain-size fractions are well reproduced. The mean coefficient of determination increases only slightly for models with more than three end-members. Thus, the goodness-of-fit statistics suggests that the three-end-member model provides a reasonable solution in that it also fulfills the requirement of a *minimum number of end-members* and *reproducibility* (Prins and Weltje, 1999; Weltje, 1997).

### Grain-size distribution and interpretation of end-members.

The three end-members that we obtained are different in that the coarser end-members (EM1 and EM2) have a dominant mode and a well-sorted distribution whereas the mode of the finer end-member (EM3) is badly defined (from 3 to 9  $\mu\text{m}$ ), which is indicative of a poorly sorted distribution (Fig. 3). Interpretation of the end-members is not straightforward and needs the consideration of the most likely mechanisms that may have acted during transport and deposition of the lithogenic sediment particles (i.e., sorting by bottom currents as well as eolian and fluvial transportation processes).

Analysis of current meter data obtained in the Alboran Sea illustrates the lack of strong deep-water currents in the area. According to these measurements western Mediterranean deep water (WMDW) at present flows at an average of 3–4  $\text{cm} \cdot \text{s}^{-1}$ ; maximum flow speeds in average may reach 20  $\text{cm} \cdot \text{s}^{-1}$  (Fabr es *et al.*, 2002). Following McCave *et al.* (1995) we have compared the carbonate-free grain-size record and the grain-size record of the total sediment fraction (Fig. 2b, 2c). The very different structure of the two records excludes bottom currents as a primary sorting mechanism at the site of our sediment core during the time period considered here. We can thus safely conclude that the grain-size variations represented by the three end-members are reliable indicators of differences in origin of the terrigenous particles contributed to the core site.

Airborne dust in deep-sea sediments is generally believed to be contained in the sediment fraction  $>6\text{--}7 \mu\text{m}$  (Sarnthein *et al.*, 1981). We use the present-day Saharan dust grain-size distribution from the red rainfall event in 1991 as a reference for comparison with the three end-members that we infer from our down-core grain-size data (Fig. 3d). The grain-size distribution of this specific Saharan dust sample is very similar to the results reported by Guerzoni *et al.* (1997) for the Mediterranean region. The mode of the sample of 10–15  $\mu\text{m}$  is very close to the mode of EM1 and quite similar to EM2. Along the core the EM2 is dominant throughout ( $\approx 60\%$  average; Fig. 3e). Therefore, it seems unlikely for EM2 to represent eolian dust. This interpretation can be tested by calculating the eolian flux using an average sedimentation rate of 0.034  $\text{cm} \cdot \text{yr}^{-1}$  that is implied by the age model of the core (Cacho *et al.*, 1999). The resulting EM2 flux of  $\approx 90 \text{ g} \cdot \text{m}^{-2} \cdot \text{yr}^{-1}$  is some four times higher than the dust flux measured by D az-Hern andez and Miranda Hern andez (1997) in southern Iberia. Therefore, EM2 is unlikely to be indicative of eolian input. EM1 much better represents the variability of eolian input as its relative contribution and flux values of 12% and 18  $\text{g} \cdot \text{m}^{-2} \cdot \text{yr}^{-1}$  respectively are in the range of modern values.

EM3, with a median size  $<6 \mu\text{m}$ , likely represents the finest sediment supplied by rivers. Irregular and intense winter precipitation events characteristic of the Alboran Sea's northern watershed, in combination with the scarce vegetation cover, mobilize large amounts of silt-sized sediments that are finally transported to and deposited in the Alboran basin. The intermediate end-member (EM2) may also result from the watershed of the Alboran Sea when rains are strong. Torrential rains could lead

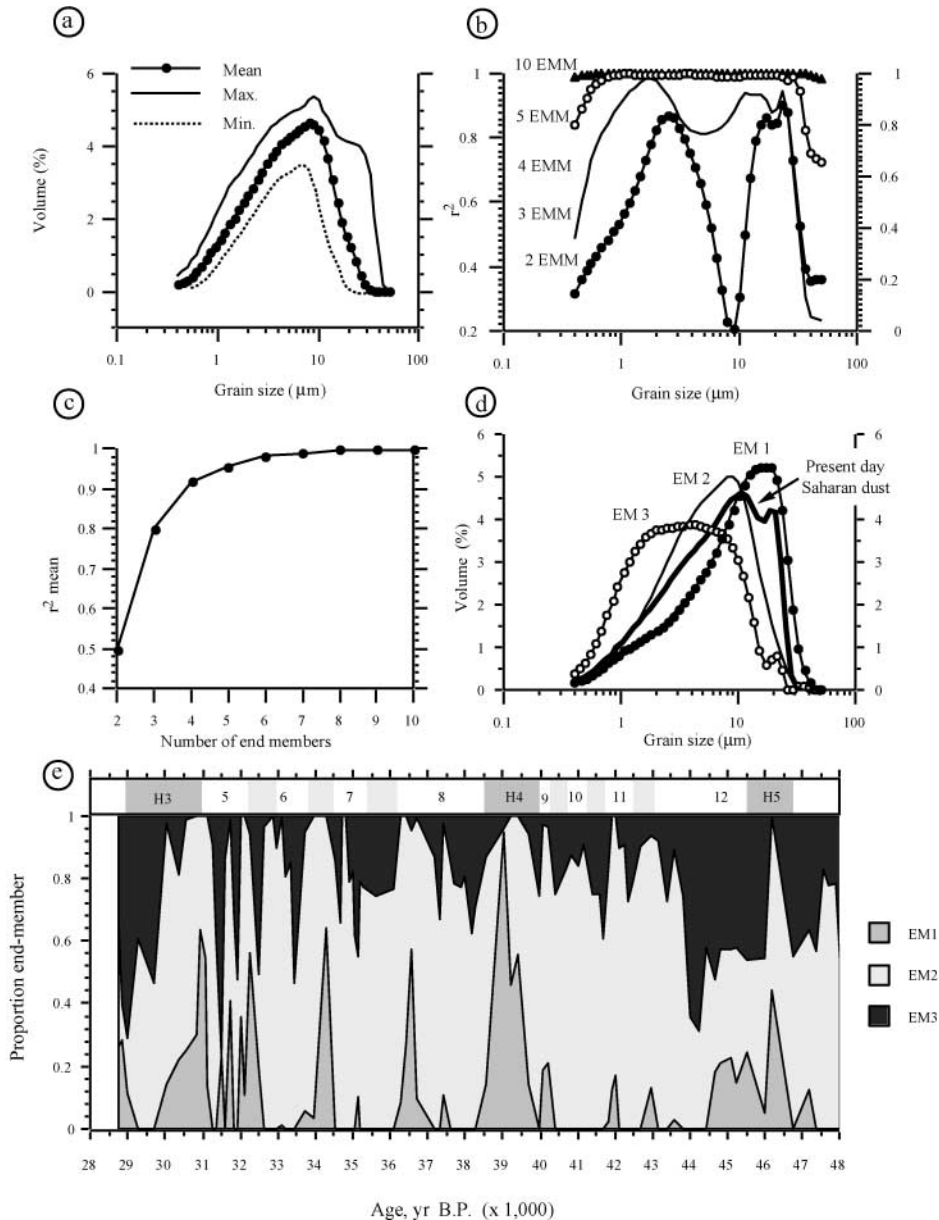


**FIG. 3.** End-member modelling results of grain-size data of core MD 95-2043. (a) Maximum, mean and minimum frequencies recorded in each size class; (b) coefficients of determination ( $r^2$ ) plotted against grain-size for different end-member solutions (2, 3, 4, 5 and 10 EM); (c) mean coefficient of determination versus the number of end-members (see text for explanation); (d) grain-size distributions for the end-members of the three end-member solution. Present-day Saharan dust grain-size distribution is also shown. (e) Time series of EM1, EM2 and EM3 relative abundance.

to the presence of coarser fluvial particles in the sediments in response to more vigorous continental runoff. Therefore, both EM2 and EM3 likely represent fluvially transported sediments, one related to the finest fraction and the other to the coarser silt particles supplied to the basin after torrential rains.

Our interpretation of the three end-members is in agreement with the sorting index record (Fig. 2e) in that periods with frequent eolian events are coeval with poorly sorted terrigenous sediments because of the apparent mixing between eolian and fluvial particles (clearly shown for HE4). Therefore, the down-

core particle size distribution agrees well with the hypothesis of a sustained fluvial sediment input during the period 48,000–28,000 cal yr B.P. that was punctuated occasionally by pulses of enhanced eolian contributions.

#### *Si/(Si + K) Index for Fluvial versus Eolian Inputs*

Saharan dust is well known for its elevated quartz contents (Guieu and Thomas, 1996), thus enabling silicon (Si) abundances to be used as an indicator of dust input. Since biogenic

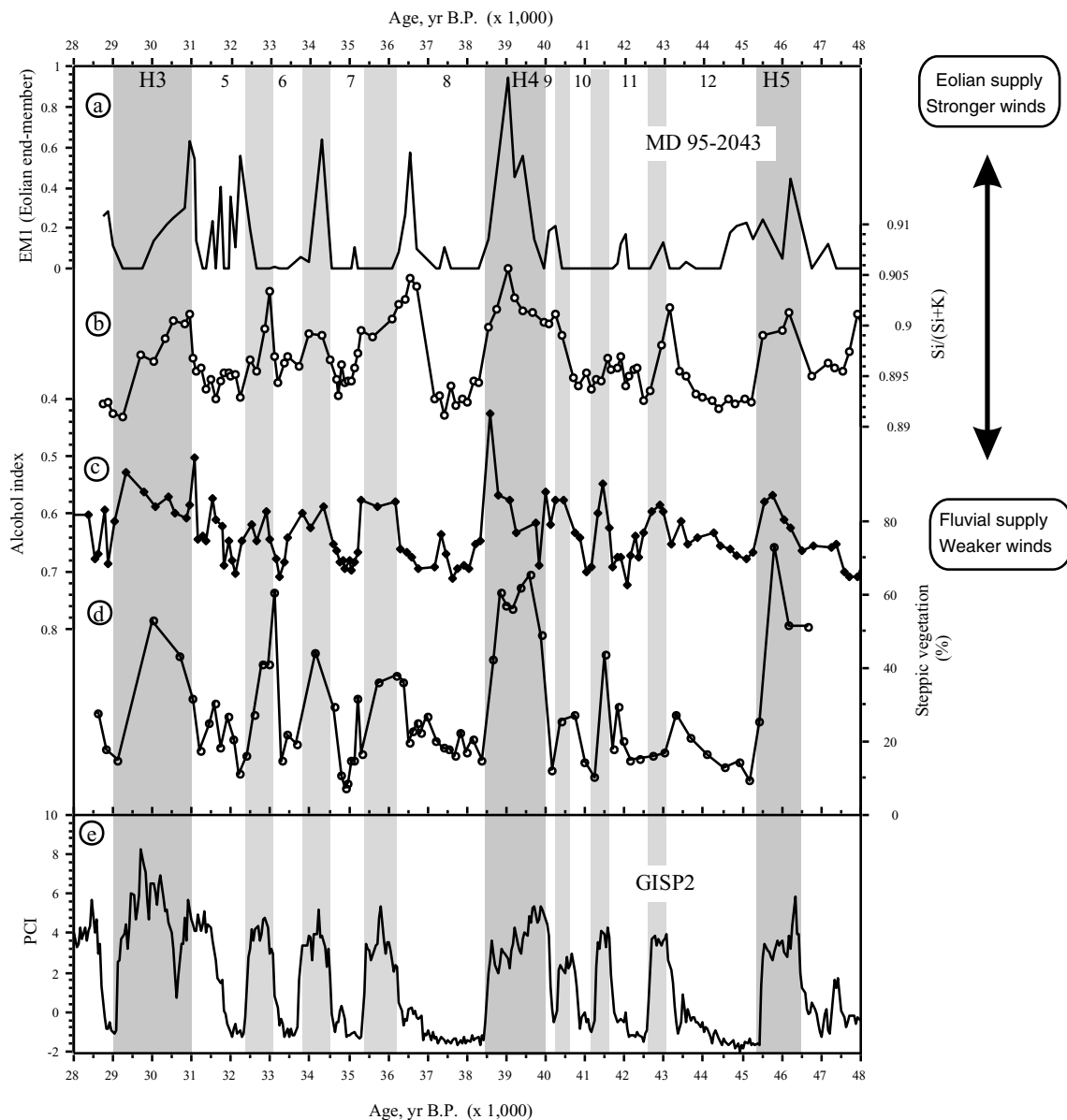


**FIG. 4.** MD 95-2043 time series of wind- and aridity-related proxies: (a) proportional contribution of the eolian end-member, (b)  $\text{Si}/(\text{Si} + \text{K})$  ratio, (c) alcohol index  $n$ -hexacosanol/ $n$ -hexacosanol +  $n$ -nonacosane from Cacho *et al.*, (2000), and (d) steppic vegetation abundance from Sánchez-Goñi *et al.* (2002) compared with (e) the Polar Circulation Index (PCI) calculated in GISP2 ice core (Mayewski *et al.*, 1994).

opal contents are very low in Alboran Sea sediments (Masqué *et al.*, 2002) we assume here the total Si content of the bulk sediments to represent the total terrigenous input. Fluvially delivered clays, notably illite, are potassium (K) enriched and thus we apply the  $\text{Si}/(\text{Si} + \text{K})$  ratio as an index to assess the relation between eolian and fluvial sediment contributions. The  $\text{Si}/(\text{Si} + \text{K})$  index is expected to be related to the mixing between the eolian and fluvial components as well as variations in the grain-size of the terrigenous material.

The  $\text{Si}/(\text{Si} + \text{K})$  index along core MD95-2043 follows the same pattern of variation as the grain-size records in that the

$\text{Si}/(\text{Si} + \text{K})$  maxima correlate with maximum values in the eolian end-member EM1 during the cold phases of the D/O cycles, a pattern that is particularly well developed during the time interval 28,000–40,000 cal yr B.P. (Fig. 4a, 4b). To date there is no evidence reported of changes in the extension of the Sahara desert belt at millennial timescales. Therefore, from our data we cannot distinguish between increases of wind intensity as the ultimate cause for increased  $\text{Si}/(\text{Si} + \text{K})$  values or expansion and increasing proximity of Saharan dust sources during the D/O stadials. However, modeling studies consistently indicate that the changes dust deposition off Africa are primarily driven by

dust transport and not so much by increased aridity in the dust source region (Mahowald *et al.*, 1999). We take this as circumstantial evidence that both proxies, the EM1 and the Si/(Si + K) ratio primarily monitor changes in eolian dust transport driven by varying wind intensity.

## DISCUSSION

Past terrigenous input of lithogenic components to the Alboran Sea are the result of eolian and fluvial sediment supply. The records of both components along IMAGES Core MD-95-2043 exhibit a millennial-scale cyclicality that shows a close structural relation to D/O climatic cyclicality seen in the Greenland ice core records. Comparison of the grain-size and geochemical records from core MD95-2043 with the down-core variability of other marine and terrestrial proxies along the same core enables to investigate the timing and the mechanisms involved in these millennial climatic changes.

### *Glacial-Wind Regimes in the Western Mediterranean Region*

Abrupt changes occur within the grain size and geochemical records that suggest higher dust transports from the Saharan region to the Alboran Sea occurred during cold stadial periods of the D/O cycles (Fig. 4a, 4b). Similar increases in dust (and salt) transport are documented in the Greenland ice records, notably the Polar Circulation Index (PCI, Fig. 4c; Mayewski *et al.*, 1994) which suggests an intensification of the Northern Hemisphere atmospheric circulation during the cold stadial phases, a contention that is further supported by coeval increases in loess deposition in Asia (An, 2000; Porter and Zhiseng, 1995) and by monsoon records (Leuschner and Sirocko, 2000; Schulz *et al.*, 1998). Within the Western Mediterranean Sea, similar intensification of wintertime northwesterly winds has been inferred that resulted in an increased rate of formation of WMDW (Cacho *et al.*, 2000; Rohling *et al.*, 1998). Such changes in WMDW ventilation are particularly well documented in the down-core record of the alcohol index along core MD95-2043 (Fig. 4c; Cacho *et al.* 2000). This index represents the relationship between two molecular biomarkers (*n*-hexacosanol and *n*-nonacosane) that have the same terrestrial source but follow different pathways of degradation behavior in the water column and sediments. Comparison of Saharan wind proxies (Fig. 4a, 4b) with those from higher latitude wind systems (Fig. 4c, 4e) illustrates the co-occurrence of increased wind strength during the cold phases over a wide latitudinal range. We can thus infer that both wind systems, the high-latitude northwesterlies and the low-latitude Saharan winds, display a similar pattern of variation during the last glacial period. Together with a coeval intensification of atmospheric transports over Greenland, this suggests a close mechanistic linking of glacial atmospheric circulation across the latitudes.

At present, atmospheric pressure gradients over the North Atlantic region that are driving the NAO system exert primary

control on dust transports from the Saharan region, with dust transports being increased during phases of increased pressure gradients (high-NAO index; Moulin *et al.*, 1997). On NAO-related timescales, variations in Sahel rainfall over the last century are highly correlated with colder SST in the North Atlantic Ocean (Folland *et al.*, 1986) thus pointing to an ocean–climate teleconnection between the high and low latitudes. Similar links between North Atlantic oceanography and climatic conditions over the Sahel zone have been observed for Holocene period in paleoclimatic records. A coexistence of cold North Atlantic and warm South Atlantic SST with periods of severe drought in the Sahara zone is documented in several paleoclimatic records from continental Africa (Lamb *et al.*, 1995; Street-Perrot *et al.*, 2000). In addition, numerical modeling points to a close linking between cold North Atlantic SST and mean annual cooling and increased aridity in subtropical Africa (deMenocal, 1995). Cooling of North Atlantic SSTs also strengthens the subtropical Atlantic high-pressure cell, thus causing dust transports from the Saharan desert to be increased. A range of paleoclimatic evidence points to an increase in Sahelian aridity and meridional dust transports during periods of colder SST in the North Atlantic.

Our records provide compelling evidence that this cross-latitude teleconnection also operated during the last glacial period and that it was particularly sensitive to the D/O climatic oscillations. In fact, evidence has been presented that the decreased northward marine heat transport during HE and the cold D/O stadial periods resulted in a warming of the tropical Atlantic (Rühlemann *et al.*, 1999) thereby increasing the meridional temperature gradient between the cold high-latitude and the warm tropical Atlantic. Applying the modern concepts of atmospheric circulation and environmental controls on atmospheric pressure gradients, this should have resulted in an increased intensity of the northwesterly wind system (Schiller *et al.*, 1997). The invasion of extremely cold surface waters during these periods into the Mediterranean Sea (Cacho *et al.*, 1999) would have further enhanced the influence of the northwesterlies on western Mediterranean climates. These meteorological conditions would have caused enhanced aridity (Street-Perrot *et al.*, 2000), more intense Saharan winds (Moulin *et al.*, 1997) and, ultimately, increased meridional transport of Saharan dust to the Alboran Sea. The potential role of such a mechanism for driving glacial climatic variability at millennial timescales has been postulated in several studies (i.e., Sánchez-Goñi *et al.*, 2002) but the details remain unclear because the influence of the large glacial ice caps over North America and Europe also play a part in modifying the atmospheric dynamics over the North Atlantic region. Nevertheless, the sedimentological and geochemical records of core MD95-2043, notably their linking with atmospheric circulation patterns, suggest that NAO-type atmospheric patterns may have caused the down-core pattern of variability of eolian sediment transports to the Alboran Sea.

## Heinrich Events & Dansgaard-Oeschger stadial periods

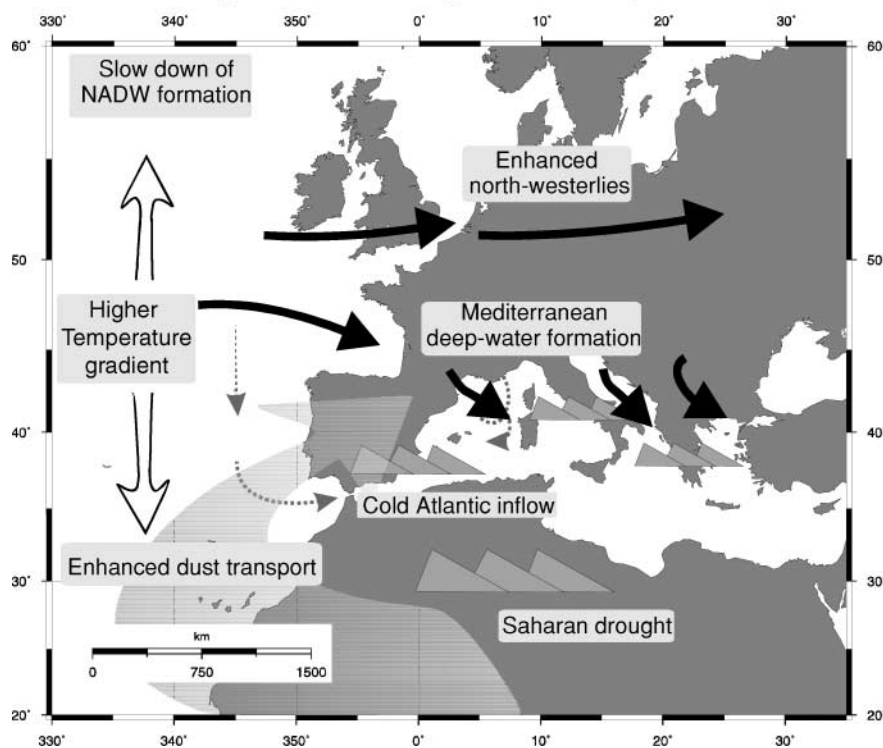


FIG. 5. Synoptic model that summarises the main processes and features that controlled the Alboran record during HE and D/O stadial periods.

### Glacial-Precipitation Patterns in the Western Mediterranean Sea

Climatic conditions in the Alboran borderlands during the last glacial period have been studied previously using pollen records from core MD95-2043 (Sánchez-Goñi *et al.*, 2002). Oscillations of atmospheric moisture contents between more arid and more humid conditions have been inferred from alternating dominance of steppic pollen taxa during the cold D/O stadial periods and deciduous and evergreen *Quercus* pollen during the warmer D/O interstadial periods. Arid conditions were especially extreme during the HE that constitute the most extreme cold events, as is illustrated by the maximum abundance of steppic or semidesert vegetation pollen (*Artemisia*, *Chenopodiaceae*, *Ephedra*) (Fig. 4d). These vegetation changes occurred rapidly, within 150 yr or less, and occurred in parallel with severe cooling of Alboran SST. Sánchez-Goñi *et al.* (2002) have proposed that a glacial atmospheric oscillation similar to the present-day NAO system was the primary driving force behind pluvial conditions on the Iberian Peninsula. It thus appears conceivable to infer that arid and cold climatic conditions that are documented in our records during the D/O stadial periods were caused by a rapid and prolonged change in atmospheric patterns that were similar to today's high NAO index patterns. Such inferences are further supported by pollen records from terrestrial

sequences in Italy and Greece that show a dominance of dry conditions during D/O stadial periods over the entire Mediterranean region (Allen *et al.*, 1999; Tzedakis, 1999). The correlation of our proxies of wind intensity and pollen data points to southern Iberia aridity variations in association with transport intensity changes as the most viable candidates to explain the D/O variability in our record (Fig. 5).

### CONCLUSIONS

Geochemical records of terrigenous contributions to the Alboran Sea sediments have been established along IMAGES Core MD95-2043 to evaluate the variation of fluvial versus eolian inputs during the last 28,000–48,000 cal yr B.P. The records display a down-core variability that is similar in structure to the D/O climatic variability seen in the Greenland ice-core records. The data indicate an increase of Saharan wind intensity during D/O stadial periods and the Heinrich events. Existing pollen records along the same core, notably increased abundances of steppic pollen taxa, indicate enhanced aridity on the southern Iberian Peninsula during these periods. This combined proxy pattern provides compelling evidence for a highly sensitive response of the low-latitude atmospheric system to the D/O climatic cycles.

We suggest that the observed proxy pattern is best explained by a variability in wind systems and precipitation patterns over the Mediterranean region that was driven by rapid switches between two modes of atmosphere circulation over the North Atlantic region. In one mode atmospheric pressure gradients in the North Atlantic region were high so that northwesterly wind intensity over the Mediterranean area was increased. This mode would arise in response to decreased North Atlantic SST that was driven by a slowdown thermohaline overturn and decreased northward marine heat transport during D/O stadial periods and the Heinrich events. This would have favored both drier conditions and more intense Saharan winds, which ultimately resulted in increased meridional transport of Saharan dust. We therefore suggest that records of eolian and fluvial sediment supply that we generated for the Alboran Sea are best explained by an atmospheric pressure gradient seesaw similar to today's North Atlantic Oscillation system. This glacial atmospheric oscillator operated on a millennial timescale causing prolonged states of climate that are very similar to the much shorter periods of today's NAO extremes.

#### ACKNOWLEDGMENTS

We thank Anna Avila (CREAF, Barcelona) for providing present-day aerosol samples to carry out grain-size analyses and E. Seguí (XRF laboratory) and M. Guart (sedimentological laboratory) for their help in laboratory analyses. We also thank Paul Mayewski for providing the PCI data from core GISP2. Dr. E. J. Rohling and J. R. M. Allen reviewed the manuscript and provided helpful suggestions. We are likewise grateful to Dr. R. Zahn for his discussion and help with improving the English. This study was supported by the IMAGES program and a Comissionat d'Universitats i Recerca fellowship (Ana Moreno). I.C. also thanks funding from EC (contract HPMF-CT-1999-00402). GRC Geociencies Marines is funded by Generalitat de Catalunya through its excellency research groups program.

#### REFERENCES

- Allen, J. R. M., Brandt, U., Brauer, A., Hubberten, H. W., Huntley, B., Keller, J., Kraml, M., Mackensen, A., Mingram, J., Negendank, J. F. W., Nowaczyk, N. R., Oberhänsli, H., Watts, W. A., Wulf, S., and Zolitschka, B. (1999). Rapid environmental changes in southern Europe during the last glacial period. *Nature* **400**, 740–743.
- An, Z. (2000). The history and variability of the East Asian paleomonsoon climate. *Quaternary Science Reviews* **19**, 171–187.
- Avila, A. (1996). Time trends in the precipitation chemistry at a montane site in Northeastern Spain for the period 1983–1994. *Atmospheric Environment* **30**, 1363–1373.
- Béthoux, J. P. (1979). Budgets of the Mediterranean Sea. Their dependence on the local climate and on the characteristics of the Atlantic waters. *Oceanologica Acta* **2**, 157–163.
- Boyle, E. (2000). Is ocean thermohaline circulation linked to abrupt stadial/interstadial transitions? *Quaternary Science Reviews* **19**, 255–272.
- Broecker, W. S. (1994). Massive iceberg discharges as triggers for global climate change. *Nature* **372**, 421–424.
- Cacho, I., Grimalt, J. O., Pelejero, C., Canals, M., Sierro, F. J., Flores, J. A., and Shackleton, N. J. (1999). Dansgaard-Oeschger and Heinrich event imprints in Alboran Sea temperatures. *Paleoceanography* **14**, 698–705.
- Cacho, I., Grimalt, J. O., Sierro, F. J., Shackleton, N. J., and Canals, M. (2000). Evidence for enhanced Mediterranean thermohaline circulation during rapid climatic coolings. *Earth and Planetary Science Letters* **183**, 417–429.
- deMenocal, P. (1995). Plio–Pleistocene African climate. *Science* **270**, 53–59.
- Díaz-Hernández, J. L., and Miranda Hernández, J. M. (1997). Tasas de deposición de polvo atmosférico en un área semiárida del entorno Mediterráneo occidental. *Estudios Geológicos* **53**, 211–220. [In Spanish]
- Dickson, B. (1997). From the Labrador Sea to global change. *Nature* **386**, 649–650.
- Ditlevsen, P. D., Svensmark, H., and Johnsen, S. J. (1996). Contrasting atmospheric and climate dynamics of the last-glacial and Holocene periods. *Nature* **379**, 810–812.
- Fabrés, J., Calafat, A., Sánchez-Vidal, A., Canals, M., and Heussner, S. (2002). Composition and spatio-temporal variability of particle fluxes in the Western Alboran Gyre, Mediterranean Sea. *Journal of Marine Systems* **33–34**, 431–456.
- Folland, C. K., Palmer, T. N., and Parker, D. E. (1986). Sahel rainfall and worldwide sea temperatures, 1901–85. *Nature* **320**, 602–607.
- Fuhrer, K., Wolff, E. W., and Johnsen, S. J. (1999). Timescales for dust variability in the Greenland Ice Core Project (GRIP) ice core in the last 100,000 years. *Journal of Geophysical Research* **104**, 31,043–31,052.
- Ganopolski, A., and Rahmstorf, E. (2001). Rapid changes of glacial climate simulated in a coupled climate model. *Nature* **409**, 153–158.
- Ganor, E., and Foner, H. A. (1996). The mineralogical and chemical properties and the behaviour of aeolian Saharan dust over Israel. In “The Impact of Desert Dust Across the Mediterranean” (S. Guerzoni and R. Chester, Eds.), pp. 163–172. Kluwer Academic, Dordrecht.
- Guerzoni, S., Molinaroli, E., and Chester, R. (1997). Saharan dust inputs to the western Mediterranean Sea: Depositional patterns, geochemistry and sedimentological implications. *Deep Sea Research II* **44**, 631–654.
- Guiu, C., and Thomas, J. (1996). Saharan aerosols: From the soil to the ocean. In “The Impact of Desert Dust across the Mediterranean” (S. Guerzoni and R. Chester, Eds.), pp. 207–216. Kluwer Academic, Dordrecht.
- Hurrell, J. W. (1995). Decadal trends in the North Atlantic Oscillation: Regional temperatures and precipitation. *Science* **269**, 676–679.
- Lamb, H., Gasse, F., Benkaddour, A., El Hamouti, N., Van der Kaars, S., Perkins, W. T., Pearce, N. J., and Roberts, C. N. (1995). Relation between century-scale Holocene arid intervals in tropical and temperate zones. *Nature* **373**, 134–137.
- Lamy, F., Hebbeln, D., and Wefer, G. (1998). Late Quaternary precessional cycles of terrigenous sediment input off the Norte Chico, Chile (27.5S) and palaeoclimatic implications. *Palaeoecography, Palaoclimatology, Palaecology* **141**, 233–251.
- Leuschner, D. C., and Sirocko, F. (2000). The low-latitude monsoon climate during Dansgaard–Oeschger cycles and Heinrich Events. *Quaternary Science Reviews* **19**, 243–254.
- Mahowald, N., Kohfeld, K., Hansson, M., Balkanski, Y., Harrison, S. P., Prentice, I. C., Schulz, M., and Rodhe, H. (1999). Dust sources and deposition during the last glacial maximum and current climate: A comparison of model results with paleodata from ice cores and marine sediments. *Journal of Geophysical Research* **104**, 15,895–15,916.
- Masqué, P., Fabrés, J., Calafat, A., Sánchez-Cabeza, J. A., Sánchez-Vidal, A., Bruach, J. M., Cacho, I., and Canals, M. (2002). Sediment accumulation rates and main sedimentological patterns of recent sediments (100 y) from the Alboran Sea. *Marine Geology*, in press.
- Mayewski, P. A., Meeker, L. D., Whitlow, S., Twickler, M. S., Morrison, M. C., Bloomfield, P., Bond, G., Alley, R. B., Gow, A. J., Grootes, P., Meese, D. A., Ram, M., Taylor, K. C., and Wumkes, W. (1994). Changes in atmospheric circulation and ocean ice cover over the North Atlantic during the last 41,000 years. *Science* **263**, 1747–1751.

- McCave, I. N., Manighetti, B., and Robinson, S. G. (1995). Sortable silt and fine sediment size/composition slicing: Parameters for palaeocurrent speed and palaeoceanography. *Paleoceanography* **10**, 593–610.
- McManus, J. (1988). Grain size determination and interpretation. In “Techniques in Sedimentology” (M. E. Tucker, Ed.), pp. 63–85. Blackwell Sci., Oxford.
- Meese, D. A., Gow, A. J., Alley, R. B., Zielinski, G. A., Grootes, P., Ram, M., Taylor, K. C., Mayewski, P. A., and Bolzan, J. F. (1997). The Greenland Ice Sheet Project 2 depth-age scale: Methods and results. *Journal of Geophysical Research* **102**, 26411–26423.
- Moulin, C., Lambert, C. E., Dulac, F., and Dayan, U. (1997). Control of atmospheric export of dust from North Africa by the North Atlantic Oscillation. *Nature* **387**, 691–694.
- Peterson, L. C., Haug, G. H., Hughen, K. A., and Röhl, U. (2000). Rapid changes in the hydrologic cycle of the tropical Atlantic during the Last Glacial. *Science* **290**, 1947–1951.
- Porter, S. C., and Zhisheng, A. (1995). Correlation between climate events in the North Atlantic and China during the last glaciation. *Nature* **375**, 305–308.
- Prins, M., and Weltje, G. J. (1999). End-member modeling of siliciclastic grain-size distributions: The late Quaternary record of eolian and fluvial sediment supply to the Arabian Sea and its paleoclimatic significance. In “Numerical Experiments in Stratigraphy: Recent Advances in Stratigraphic and Sedimentological Computer Simulations,” pp. 91–111. SEPM Special Publications.
- Rodó, X., Baert, E., and Comin, F. A. (1997). Variations in seasonal rainfall in Southern Europe during the present century: relationships with the North Atlantic Oscillation and the El Niño-Southern Oscillation. *Climate Dynamics* **13**, 275–284.
- Rodríguez, S., Querol, X., Alastuey, A., Kallos, G., and Kakaliagou, O. (2001). Saharan dust contributions to PM10 and TSP levels in Southern and Eastern Spain. *Atmospheric Environment* **35**, 2433–2447.
- Rohling, E. J., Hayes, A., Rijk, D., Kroon, D., Zachariasse, W. J., and Eisma, D. (1998). Abrupt cold spells in the northwest Mediterranean. *Paleoceanography* **13**, 316–322.
- Romero, R., Sunner, G., Ramis, C., and Genovés, A. (1999). A classification of the atmospheric circulation patterns producing significant daily rainfall in the Spanish Mediterranean area. *International Journal of Climatology* **19**, 765–785.
- Rühlemann, C., Mulitza, S., Müller, P., Wefer, G., and Zahn, R. (1999). Warming of the tropical Atlantic Ocean and slowdown of thermohaline circulation during the last deglaciation. *Nature* **402**, 511–514.
- Sánchez-Goñi, M. F., Cacho, I., Turon, J. L., Guiot, J., Sierro, F. J., Peyrouquet, J.-P., Grimalt, J. O., and Shackleton, N. J. (2002). Synchronicity between marine and terrestrial responses to millennial scale climatic variability during the last glacial period in the Mediterranean region. *Climate Dynamics* **19**, 95–105.
- Sarnthein, M., Tetzlaff, G., Koopmann, B., Wolter, K., and Pflaumann, U. (1981). Glacial and interglacial wind regimes over the eastern subtropical Atlantic and North-West Africa. *Nature* **293**, 193–196.
- Schiller, A., Mikolajewicz, U., and Voss, R. (1997). The stability of the North Atlantic thermohaline circulation in a coupled ocean-atmosphere general circulation model. *Climate Dynamics* **13**, 325–347.
- Schulz, H., von Rad, U., and Erlenkeuser, H. (1998). Correlation between Arabian Sea and Greenland climate oscillations of the past 110,000 years. *Nature* **393**, 54–57.
- Street-Perrot, F. A., Holmes, J. A., Waller, M. P., Allen, M. J., Barber, N. G. H., Fothergill, P. A., Harkness, D. D., Ivanovich, M., Kroon, D., and Perrot, R. A. (2000). Drought and dust deposition in the west African Sahel: A 5500-year record from Kakemaru Oasis, northeastern Nigeria. *The Holocene* **10**, 293–302.
- Sumner, G., Homar, V., and Ramis, C. (2001). Precipitation seasonality in Eastern and Southern coastal Spain. *International Journal of Climatology* **21**, 219–247.
- Tzedakis, C. (1999). The last climatic cycle at Kopais, central Greece. *Journal of Geological Society of London* **156**, 425–434.
- Weltje, G. J. (1997). End-member modeling of compositional data: Numerical-statistical algorithms for solving the explicit mixing problem. *Journal of Mathematical Geology* **29**, 503–549.
- Zahn, R., Schönfeld, J., Kudrass, H. R., Park, M. H., Erlenkeuser, H., and Grootes, P. (1997). Thermohaline instability in the North Atlantic during meltwater events: Stable isotope and ice-rafted detritus records from core S075-26KL, Portuguese margin. *Paleoceanography* **12**, 696–710.